

Equivalence between the methods established by ISO 15927-3 to determine wind-driven rain exposure: Reanalysis and improvement proposal

José M. Pérez-Bella^{a,*}, Javier Domínguez-Hernández^a, Enrique Cano-Suñén^a, Mar Alonso-Martínez^b,
Juan J. del Coz-Díaz^b

^a *Department of Construction Engineering, Engineering and Architecture School, University of Zaragoza, María de Luna, s/n, 50018 Zaragoza, Spain.*

^b *Department of Construction Engineering, University of Oviedo, Edificio Departamental Viesques nº 7, 33204 Gijón, Spain.*

Abstract

ISO standard 15927-3 establishes two calculation methods to characterise wind-driven rain exposure on building façades, with different approximations according to the available climatic data: (i) a reference method, using hourly wind and rain data, and (ii) an alternative method using average wind records and the present weather code for rain in half-day intervals when hourly data are not available. However, the equivalence between the two methods was only validated in three British cities with similar environmental conditions (London, Manchester, and Edinburgh), and for only four façade orientations. In addition, the description of the second method also admits different interpretations that can influence its results. This study re-examines the real equivalence between the two methods, comparing their results in multiple façade orientations of 12 Spanish locations subjected to varied amounts of wind-driven rain exposure. The analysis shows that the reliability of the method based on non-hourly data varies significantly according to the methodological interpretation applied, making it advisable to review its current description. Finally, an improvement is proposed that reinforces the equivalence and reliability of the alternative method with respect to the reference method, regardless of the climate of the analysed location.

Keywords

Wind-driven rain; ISO standard; Climate data; Façade design; method reliability

* Corresponding author. Department of Construction Engineering, University of Zaragoza (UZ), María de Luna, s/n, 50018, Zaragoza, Spain. Tel.Fax: +34 976 76 21 00.
E-mail address: jmpb@unizar.es (José M. Pérez-Bella)

1. Introduction

The penetration of rainwater into building façades causes multiple types of deterioration in porous construction materials (such as frost attack, salt migration, crystallisation stress, cracking, and loss of adherence), reductions in the efficiency of the thermal insulation of the building envelope, impacts on the health conditions of residents, and biodeterioration phenomena [1-8]. The wind-deflected rain that impacts the vertical surface of the façades (wind-driven rain (WDR)) is the main source of moisture for this penetration process [9-10]. Accurately determining the exposure of each façade to the rainwater supply is therefore a key aspect for defining watertight designs.

ISO standard 15927-3 constitutes an international reference for the calculation of this exposure, and enables the WDR that would impact on a given façade orientation to be quantified. This is totalled over one year, and over the worst WDR period likely to occur in any given 3-year period [11-15]. Accordingly, the standard uses hourly rainfall and wind velocity data (i.e., speed and direction) collected at the sites for a minimum of 10 years. This calculation procedure is based on the methodology applied by BS standard 8104, but it does not include the WDR maps and directional roses included in the British standard, and is thus applicable to any geographic area (hereafter termed the reference method) [16].

In turn, this standard incorporates an alternative method for locations without hourly climate data, which uses average wind records and the present weather code defined by the World Meteorological Organization [17]. This method (hereafter termed the alternative method) characterises periods when the façade is likely to moisten. This means it does not quantify the amount of water that impacts the façade, but the severity of these ‘wetting periods’. For this purpose, each 12 h interval (‘half-day’) is assigned a wetting (+1), drying (-1) or neutral nature (0), according to the presence and intensity of the rainfall, mean wind speed, wind direction and relative humidity during each half-day. The number of wetting half-days accumulated during a single wetting period that might be exceeded once every 10 years should

provide *a priori* a WDR exposure characterisation on a given façade orientation equivalent to the reference method [11].

Sanders analysed the equivalence between the results of both methods at several British locations (cooperative project IEA-Annex 41 of the International Energy Agency), and this comparison was graphically collected in the Informative Annex D of the standard ISO 15927-3 [11, 18]. However, neither the number of sites studied (London, Manchester, and Edinburgh airports, three cities with a similar rainfall amount of between 600 and 830 mm/year) nor the orientations analysed (North, South, East, and West) are sufficiently representative to validate the equivalence between the two calculation methods [19]. Furthermore, the description of the alternative method does not define how to identify the end of each period of accumulated wetting half-days, thus allowing different interpretations that could lead to different results.

To address this issue, this research assesses the real equivalence between the two calculation methods by analysing a representative number of locations and façade orientations, subjected to varied climates and WDR exposures. Accordingly, 12 Spanish locations distributed throughout the regions of Galicia (northwest of the Iberian Peninsula), La Rioja (Ebro river valley), and the Canary Islands were studied. These regions have average rainfall amounts ranging from 72 mm/year to 1,734 mm/year, mean wind speeds ranging from 1.2 m/s to 6.4 m/s, and climates ranging from hot desert to oceanic [20-21].

This reanalysis will allow the reliability of the alternative method to be quantified under different climatic conditions, discuss the validity of different methodological interpretations and identify the one that is capable of achieving better agreement with respect to the reference method. Finally, an improvement for this alternative method is proposed. This advancement of the international ISO standard 15927-3 will provide a more reliable characterisation of the WDR exposure in locations without simultaneous records of hourly climatic data, thus enabling more suitable designs for building façades in these locations.

2. Background. Description of standard ISO 15927-3

The reference method of ISO standard 15927-3 uses a semi-empirical approach to calculate the WDR exposure, based on the overall formulation established by the ‘WDR relationship’ (Eq. 1). This relationship links simultaneous records of wind speed U (m/s) and rainfall intensity R_h (mm) to obtain the water amount impinging on the vertical façade surface [22-23].

$$WDR_{\theta} = k \cdot U \cdot R_h \cdot \cos(D - \theta) \quad (1)$$

To determine the WDR_{θ} (l/m^2) on each specific façade orientation θ ($^{\circ}$), the WDR relationship incorporates a cosine projection that uses simultaneous records of the wind direction D ($^{\circ}$). This requires a different calculation for each possible façade orientation θ , and only those results with a positive value are considered (i.e., WDR impinging on the specific façade orientation). The result is adjusted by an empirical coefficient k (s/m), which varies depending on the façade geometry, building configuration, raindrop-size distribution and U and R_h values [24]. The subsequent development of this WDR relationship allowed the development of several WDR maps for the United Kingdom and culminated in a calculation standard (BS 8104) based on the use of hourly climate records [16, 25-27].

Taking this British standard as a model, ISO standard 15927-3 establishes a general method that enables a generalised calculation of the amount of WDR passing through a vertical surface in an undisturbed airstream. This represents the WDR that would occur on a given orientation façade at a height of 10 m above ground level in free field conditions. This amount can also be weighted by dimensionless coefficients (named ‘wall indices’), which represent the influence of the building shape, terrain roughness, surrounding topography, and nearby obstructions [11]. In turn, this reference method allows the WDR exposure to be quantified in two different time intervals: annually and during sustained exposure intervals (named ‘spells’).

Thus, the average annual WDR exposure on a specific orientation or $I_{A\theta}$ (mm/year) is calculated from at least 10 years of simultaneous hourly wind speed U (m/s), wind direction D ($^\circ$), and rainfall intensity R_h (mm) data in airfield conditions. Airfield conditions means a height of 10 m above ground level in an open field, as established by the World Meteorological Organization [28]. In the summation of the formula, only the m co-occurrent climatic records gathered over N years in which the wind direction D affects the analysed orientation θ (Eq. 2) are considered.

$$I_{A\theta} = \frac{2}{9} \cdot \frac{\sum_{i=1}^m U_i \cdot (R_{h_i})^{8/9} \cdot \cos(D_i - \theta)}{N} \quad (2)$$

To quantify the exposure that can accumulate during a spell, the j hourly records of wind velocity (U and D) and precipitation (R_h) during each spell (Eq. 3) are analysed, in which the wind direction D affects the analysed orientation θ [11]. Each specific spell index $I'_{S\theta}$ (mm/spell) determines the accumulated WDR on the orientation during one of these exposure intervals.

$$I'_{S\theta} = \frac{2}{9} \cdot \sum_{i=1}^j U_i \cdot (R_{h_i})^{8/9} \cdot \cos(D_i - \theta) \quad (3)$$

The ISO standard states that each spell ends with the arrival of 96 consecutive hours without WDR over the façade orientation, at which point the loss of moisture by evaporation is considered to exceed the gain from the previous WDR (Annex B of ISO 15927-3).

To obtain a single characteristic exposure value $I_{S\theta}$ (mm/spell), the most unfavourable spell index that can occur every 3-years is determined [11]. Accordingly, the ISO standard uses an approach based on traditional statistical representations (i.e., the 67th percentile of the $I'_{S\theta}$ values). However, researchers such as Orr and Viles have demonstrated how the use of these traditional percentiles is inadequate to represent extreme weather events, because the expected $I_{S\theta}$ values are significantly underestimated [15, 29-30].

2.1 The alternative method and its original validation

Currently, there are several procedures that can be used to characterise WDR exposure in locations without simultaneous records of hourly climatic data, all of them based on solid physical bases [9, 31-32]. Nevertheless, ISO standard 15927-3 supports an alternative calculation method that assesses the interval during which the façade is wet due to WDR (hereafter referred to as the ‘wetting period’) [11]. The amount of water impinging on the façade is not determined, which diminishes the physical sense of this alternative method. In any case, it is supposed that the severity of these wetting periods should show a good correlation with the results of the reference method ($I_{A\theta}$ and $I_{S\theta}$ values), making this method a functional and reliable alternative.

This alternative calculation analyses climatic data at half-day intervals, from 06 to 18 and from 18 to 06 hours. For one of these intervals to be considered a wetting half-day on the analysed façade orientation (assigning a value of +1), the following thresholds must be surpassed:

- There is more than 4 mm of precipitation.
- The mean wind speed is greater than 2 m/s.
- The average wind direction is within $\pm 60^\circ$ of the perpendicular to the façade orientation θ .
- The present weather code reports some precipitation for at least three of the five records of the half-day (at 06:00, 09:00, 12:00, 15:00, 18:00, and 18:00, 21:00, 00:00, 03:00 and 06:00, respectively).

For a half-day to be considered drying or evaporative (assigning a value of -1), the following environmental conditions must be recorded:

- The average atmospheric relative humidity is lower than 70%.
- The mean wind speed is greater than 2 m/s.
- The average wind direction is within $\pm 60^\circ$ of the perpendicular to the analysed façade orientation θ .

The half-days that do not meet these conditions are considered neutral half-days (value of 0), with an indeterminate evaporative and wetting potential. With all available half-days characterised in this way

(+1, -1, and 0), a cumulative time series is elaborated for each location and façade orientation, assuming that the façade cannot be dried below the initial level of the series (i.e., the cumulative sum has a minimum value of 0) [11]. For each year and each possible façade orientation θ , the maximum accumulated value must be identified (i.e., the maximum sum of wetting half-days in a single wetting period), which is representative of the most severe wetting period of the year.

To obtain a single reference exposure value, the maximum accumulated value that can be expected in 10 years for each orientation is calculated. To achieve this, an extreme value analysis (Gumbel distribution) is applied to calculate the value linked to a 10-year return period (Eq. 4) [33-34].

$$x = u_x - \beta_x \left(\ln \left(-\ln \left(1 - P(x \geq \gamma) \right) \right) \right) = u_x - \beta_x \left(\ln \left(-\ln \left(1 - \frac{1}{\text{Return period (years)}} \right) \right) \right) \quad (4)$$

This general equation expresses the probability P that a given value γ of the variable x (in this case the maximum accumulated value) is exceeded during a particular year, where u_x and β_x are the mode and the dispersion parameters of the distribution, respectively. Thus, in this case, both parameters depend only on the yearly maximum accumulated values and the number of years considered. This probability $P(x \geq \gamma)$ is inversely proportional to the return period associated with the value γ . For example, the annual probability of exceeding a value of the variable associated with a 10-year return period is 0.1.

It is worth clarifying that for the original validation of this alternative method, which was performed in British locations and represented in Informative Annex D of the ISO standard, not even the previous calculation criteria were applied (Fig. 1): on the Y-axis, the 90th percentile value of the $I_{A\theta}$ indices and the 93rd percentile value of the $I_{S\theta}$ indices were represented; on the X-axis, the 90th percentile value of the yearly maximum accumulated values during wetting periods was used [18].

Figure 1. Coefficients of determination identified for the original validation carried out in London (Heathrow), Manchester (Ringway), and Edinburgh (Turnhouse). *Data obtained from IEA-Annex 41 and verified with Figures D.1 and D.2 of ISO standard 15927-3.*

To analyse the equivalence between both methods in the scatter plots, a common R^2 measure of goodness-of-fit (coefficient of determination) has been determined [35]. The closer its value is to 1, the better the approximation between the results of both methods. In turn, the representation of the regression line also allows intuitive appreciation of the distance of the results that are scattered around the graphs. The same method of examination will also be maintained later to compare the reliability of the other methodological interpretations proposed.

As seen in Fig. 1, the joint R^2 values obtained for the British cities analysed are not very high, and there are also significant differences if each location is analysed separately. Further, considering the insufficient number of points represented, a rigorous analysis of the convergence between both methods is still pending.

3. Methodology

Although the alternative method aims to determine the number of wetting half-days accumulated in a single wetting period (i.e., wetting period severity), the ISO standard does not establish any rule to define the end of these wetting periods. Further, the definition applied for the spell of the reference method is not applicable because it is based on hourly records. Logically, the duration of these periods affects the number of wetting half-days accumulated in them.

After a detailed analysis of the working documents developed for IEA-Annex 41, it could be deduced that for the original validation performed between the two methods (Informative Annex D of standard ISO 15927-3 and Fig. 1), the wetting periods on each façade was arbitrarily considered to have ended after the occurrence of a single drying half-day. This means the value of the cumulative series returned to 0 when a value of -1 occurred [18]. In this sense, it is debatable that a single drying half-day can compensate for the façade moisture acquired from the previous WDR. For example, each spell of the reference method requires 96 consecutive hours without rain on the façade to be considered finished.

Therefore, other possible methodological interpretations that are compatible with the approach of the ISO standard can be proposed (Table 1):

A) The cumulative series returns to 0 when there are 8 half-days without +1 values, thus considering an approach analogous to that established for the spell of the reference method.

B) Each wetting period ends when a number of drying half-days equal to the previous wetting half-days has been accumulated, thus assuming an equivalent and opposite effect for both types of half-days.

Table 1. Summary of the methodological interpretations considered for the reanalysis of the alternative method.

As shown graphically in Fig. 2 for one of the Spanish locations analysed in this study, the methodological interpretation assumed by each practitioner can significantly alter the results obtained by using this alternative method.

Figure 2. Accumulated wetting half-days on a specific façade of Pazuengos (La Rioja) during 2008, considering three different interpretations for the wetting period length. The periods end on a drying half-day (original validation in ISO annex); A) upon 8 non-wetting half-days; and B) when the number of drying and wetting half-days are equal.

Considering all the above, the $I_{A\theta}$ and $I_{S\theta}$ values will be determined in 12 Spanish sites subjected to varied climatic conditions, considering up to 24 different façade orientations in each location (15° intervals). Taking these results based on hourly data as a reference, each of the three interpretations proposed for the alternative method will be applied (see Table 1) to identify the most accurate and reliable one. To favour a more coherent comparison between the two methods, the $I_{S\theta}$ results will also be calculated through an extreme value analysis (Gumbel distribution, Eq. 4) to homogenise the statistical estimation of both methods and obtain more realistic results of the worst spell that can occur every 3 years (i.e., 3-year return period, Table 2). Finally, a general methodological improvement for the alternative method will be proposed to reach better agreement with the reference method.

Table 2. Example of the summary of the highest annual $I'_{S\theta}$ values at the Calahorra station and the Gumbel distribution parameters required for the calculation of the $I_{S\theta}$ reference value.

3.1 Reference for comparison: Wind-driven rain results based on hourly data

The 12 selected sites are distributed across three Spanish regions characterised by different climates and WDR exposures [20-21]. The main characteristics of these weather stations and their $I_{A\theta}$ and $I_{S\theta}$ results based on hourly data are summarised in Fig. 3.

The sites analysed in the Canary Islands are located on four islands of the archipelago (Tenerife, Fuerteventura, La Gomera and Gran Canaria), which are near the coast and at an altitude less than 100 m. Hot semi-arid and hot desert climates predominate, with a mean annual rainfall that only reaches 72 mm/year (Pozo Negro station). In addition, the mountainous topography of the islands influences the direction of the prevailing winds, causing the most exposed façade orientations to vary at each station. For the WDR analysis, 30-min records of wind velocity and rainfall intensity, collected over 10 years (2008-2017) have been used [36]. These 30-min data were grouped to obtain the hourly data required by the reference method (Eqs. 2-4). The records showed occasional discontinuities due to maintenance and system failures, with a maximum of 6.12% of missing data at the Vecindario station.

The four locations of La Rioja (interior of the Iberian Peninsula) are located at higher altitudes, ranging from 328 m in Calahorra to 1,299 m in Pazuengos. Located in the Ebro river valley and its surrounding mountains, these stations are characterised by a dominant wind blowing from the North/Northwest as a consequence of the pressure gradients between the Bay of Biscay and the Mediterranean Sea [37]. In general, these sites present a temperate oceanic climate, with moderate rainfall amounts ranging from 406 mm/year (Calahorra and Cabretón) to 598 mm/year (Pazuengos). Again, 30-min records gathered between 2008 and 2017 have been analysed, and these records have been grouped to form hourly data [38].

The low-pressure areas that frequently cross Galicia (in the far northwest of the Iberian Peninsula) generate South/Southwest prevailing winds from the Atlantic Ocean that increase the rainfall of these stations (up to 1,734 mm/year in Tui station) [39]. The stations of Tui (Mt. Aloia) and Malpica de Bergantiños are near the coast, while A Fonsagrada and Verín (Vilamaior) are located inland and at higher altitudes. All stations generally have a warm Mediterranean climate, which is greatly influenced by the proximity of the ocean. In this region, 10-min records, which have been carefully grouped to form hourly series, are available [40]. The quality of these 10-min records (also compiled between 2008 and 2017) is excellent, with only 0.09% of missing data at the Verín (Vilamaior) station.

Figure 3. WDR exposure results based on hourly climatic data ($I_{A\theta}$ and $I_{S\theta}$ values) for the 12 analysed weather stations (*degrees from the North*): Canary Islands (top), La Rioja (centre), and Galicia (bottom). Their main characteristics and locations are also shown.

The stations with greater WDR exposures are in Galicia (Tui, 1,505 mm/year for orientation 225° and Malpica de Bergantiños, 644 mm/spell for orientation 270°). In Galicia, the directional exposure is also consistent with the prevailing winds during low-pressure events. In contrast, the less exposed stations are identified in the Canary Islands (Pozo Negro station, 24 mm/year and 20 mm/spell for the orientation 270°), as a consequence of their low precipitation. In all stations, the directional distribution of the $I_{S\theta}$ values coincides with that of the $I_{A\theta}$ values, presenting minimal orientation differences for the most exposed façades (Fig. 3).

In the La Rioja stations, the difference between the stations of Calahorra and Cabretón stands out because, despite their identical average rainfall (406 mm/year), they show very different $I_{A\theta}$ and $I_{S\theta}$ values as a result of their different wind exposures. A similar effect is also observed at the Galician station of Verín (Vilamaior), which presents a WDR exposure that is much lower than that of other Galician stations (as Malpica de Bergantiños, with a mean wind speed of 6.40 m/s).

4. Reanalysis of the alternative method, considering different methodological interpretations

From the same 10-min and 30-min records used with the reference method, the necessary climate series (precipitation values, average wind speed, average wind direction, atmospheric relative humidity, and occurrence of precipitation in intervals of 3 to 12 h) have been developed to apply the alternative method.

In this way, any discrepancy between the baseline data used by both methods is avoided. All results obtained by means of the alternative method for each façade orientation, location, and possible methodological interpretation are shown, given their extension, in the supplementary material to this publication and graphically in Fig. 4.

Figure 4. WDR exposure characterisation based on different interpretations of the alternative method (accumulated wetting half-days), for the 12 Spanish weather stations (*degrees from the North*).

4.1 Original validation: Each façade wetting period ends when a drying half-day occurs

The interpretation originally used to validate the alternative method (IEA-Annex 41) assumes that the occurrence of any drying half-day ends the wetting period, resetting the cumulative sum of wetting half-days to 0 [11, 18]. This contrasts with the 96 h without WDR necessary to finish a spell and discards the possibility that the accumulated dampness on the façade can be re-established shortly thereafter with the appearance of new wetting half-days.

The application of this interpretation at the 12 Spanish locations confirms its insufficient convergence with the results of the reference method: the linear regressions identified at the sites offer an average coefficient of determination R^2 of 0.6976 for the $I_{A\theta}$ values and of 0.6863 for the $I_{S\theta}$ values (Fig. 5). This average goodness-of-fit is comparable to that originally identified at the three British locations (review Fig. 1) and can cause important errors in the characterisation of the WDR exposure using the alternative method. In this way, the maximum expected accumulated value for a 10-year return period is identified at the Tui station (Mt. Aloia), reaching 91.52 wetting half-days for the 240° orientation (Fig. 4). In contrast, at the Pozo Negro station, a maximum value of only 1.88 half-days is expected before a drying half-day evaporates the moisture of the façade (orientations 255° to 330°).

In addition, the results of the 12 stations have been represented together to obtain a best-fit relationship between the reference values of accumulated wetting half-days and the $I_{A\theta}$ and $I_{S\theta}$ values (notice both joint graphs in Fig. 5). As observed, neither relationship is sufficiently reliable to reveal a general extrapolation between the results of both methods (joint R^2 values of 0.8033 and 0.7198), which is evidence for the important differences between the linear regressions of each station.

Figure 5. Coefficients of determination identified for the 12 analysed weather stations by applying the original approach supported by Informative Annex D of ISO 15927-3.

4.2 Interpretation A: Each façade wetting period ends when there are 4 days without wetting half-days

In this case, an analogous pattern to the spell considered by the reference method is proposed: the cumulative sum of wetting half-days is reset with the arrival of 8 half-days without a +1 value. Every half-day and for each façade orientation, the results of 8 half-days (the current and the next 7) have been analysed. If none of them was equal to +1, the cumulative sum for this half-day was returned to 0, thus finishing any previous wetting period. Although it is debatable whether 96 h is an ideal interval to guarantee the evaporation of moisture from any type of façade in any climate, at least this approach would standardise the definition of wetting period considered throughout the ISO standard.

In general, this interpretation identifies wetting periods equal to or less severe than the previous interpretation in all locations. Tui station (210° orientation) presents the maximum accumulated value (for a 10-year return period), reaching up to 14.73 wetting half-days (Fig. 4). Again, Pozo Negro presents the lowest results, reaching a maximum of 1.88 wetting half-days for façade orientations between 255° and 330°.

The regression analysis (Fig. 6) shows how this interpretation improves the equivalence between the two methods in several locations: the average R^2 value of the $I_{A\theta}$ values improves significantly (reaching 0.7713) and slightly in relation to the $I_{S\theta}$ values (0.7157). In any case, the disparity between the linear regressions of each location is maintained, which precludes a reliable general expression to extrapolate the results of both methods anywhere (joint R^2 value of 0.7524 and 0.6620 for the $I_{A\theta}$ and $I_{S\theta}$ values, respectively).

Figure 6. Coefficients of determination identified for the 12 analysed weather stations by applying Interpretation A.

4.3 Interpretation B: Each façade wetting period ends when the drying half-days cancel out the cumulative sum of previous wetting half-days

In this case, it is proposed that the end of each wetting period occurs when the cumulative sum of wetting half-days returns to 0 by the occurrence of an equivalent number of drying half-days. This approach can mean that in locations with few drying half-days (as in the case of Galicia), the wetting periods are prolonged indefinitely, without the cumulative sum ever returning to 0. To solve this issue, the cumulative sum is considered to restart at the beginning of each year, thus characterising the annual wetting conditions in a differentiated manner.

Regarding the previous interpretations, this approach increases the severity of the wetting periods in stations with rainy climates and causes few significant changes in dry weather stations (Fig. 4). Thus, sums of up to 105.84 wetting half-days at Tui station (210°) are identified, with Pozo Negro being the station with the less severe periods (again a maximum of 1.88 wetting half-days, 255°-330° from the North).

This simple compensation between the wetting and drying half-days provides a general improvement in equivalence with the reference method (Fig. 7), especially in relation to the $I_{S\theta}$ values (reaching an average R^2 value of 0.7775). There is also greater homogeneity between the linear regression of the locations, which enables two general expressions that reasonably accurately extrapolate the $I_{A\theta}$ and $I_{S\theta}$ values of any location from the alternative method result to be obtained (joint R^2 of 0.9118 and 0.8703, respectively).

Figure 7. Coefficients of determination identified for the 12 analysed weather stations by applying Interpretation B.

5. Discussion and improvement proposal

The disparity of the previous results demonstrates the need to review standard ISO 15927-3 to clarify the procedure that should be followed to quantify the length of the wetting periods. In turn, although Interpretation B increases the reliability and precision of the alternative method, it still does not guarantee adequate equivalence with the reference method in any situation (some poor correlations persist, such as Calahorra, Pazuengos and Vecindario). Therefore, it is necessary to propose a new methodological improvement that can ensure greater reliability of this alternative method in any situation.

5.1 Improvement proposal for the alternative method

Conceptually, it is reasonable to assume that the annual WDR exposure is related to the number of wetting half-days at the location. For this reason, the annual number of wetting half-days expected for a 10-year return period has been determined on each façade orientation of the 12 Spanish sites analysed (Fig. 4). For this calculation, the number of wetting half-days recorded each year in each orientation have

been counted, thus avoiding the definition of wetting periods and any cumulative sum. These annual totals are used as the distribution for applying Eq. 4 (analogously to the example presented in Table 2 and to the one carried out with the other methodological interpretations).

Tui (Mt. Aloia) presents the highest yearly number of expected wetting half-days, with up to 125.97 half-days for a façade orientation of 20°. Cabretón presents the opposite situation, with only 4.04 wetting half-days per year expected for the most exposed orientations (300° to 360°). Verín station, despite its high rainfall, also presents a limited number of expected wetting half-days (only 35.68 for the orientation 180°). This lesser exposure of Cabretón and Verín is also observed in all possible interpretations of the alternative method, which suggests that the threshold established for the wind velocity (i.e., greater than 2 m/s) constitutes a methodological obstacle for characterising many wetting intervals in locations with limited wind exposure.

In any case, a regression analysis confirms that this simple calculation of the expected number of wetting half-days in a year (for a 10-year return period) can provide a better equivalence with respect to the reference method compared to any of the previous interpretations of the alternative method. Thus, more reliable linear regressions are obtained, reaching an average R^2 value of 0.9226 for the $I_{A\theta}$ values (Fig. 8). Despite the obvious climatic differences, up to 9 of the 12 sites have coefficients of determination greater than 0.9, with a more homogeneous goodness-of-fit among all regions. In addition, the linear regressions of the locations are very similar, which enables a general expression for extrapolating the results between the two methods in any situation to be defined with a reasonable accuracy (joint R^2 value of 0.9273 for the $I_{A\theta}$ values).

Figure 8. Coefficients of determination identified in the 12 analysed weather stations by considering the expected annual number of wetting half-days for a 10-year return period.

This calculation of wetting half-days also provides a better equivalence with respect to the $I_{S\theta}$ values (average R^2 value of 0.8714, with 6 locations with R^2 values greater than 0.9 and none less than 0.7). However, the disparity between the linear regressions of some stations makes the joint coefficient of determination reach a value of only 0.7855, thus preventing a general extrapolation of the $I_{S\theta}$ values that is better than that achieved by Interpretation B.

In this sense, Malpica de Bergantiños presents a dispersion of results that is particularly inconsistent with the general best-fit relationship (see Fig. 8). This disruptive effect is also perceived in Figs. 5-7 for the $I_{S\theta}$ values and slightly for the $I_{A\theta}$ values. This can be explained by the environmental conditions of the site (in an exposed headland on the Atlantic coast), which are subjected to short and intense storms that cause high $I_{S\theta}$ values but also a number of wetting half-days that is comparatively lower than that of the other stations. These conditions cause their results to be dispersed in regard to those of the other stations, characterised by more uniform precipitation and a greater number of wetting half-days for a similar exposure (e.g., A Fonsagrada and Tui). The ISO standard also warns of the possible inconsistencies in its results in places characterised by strong convective storms. In any case, the proposed methodological improvement is also capable of providing a particularly high goodness-of-fit between the two methods in this type of emplacement (R^2 of 0.9505 in Malpica de Bergantiños for the $I_{S\theta}$ values).

5.2 Application recommendations

The results obtained for sites subjected to a wide variety of climates allow the following general recommendations to reformulate the alternative method supported by standard ISO 15927-3, based on average wind and the present weather code for rain:

- To characterise both the mean annual WDR exposure and the exposure associated with a period of WDR, it is more reliable to simply consider the number of expected wetting half-days in a year on each façade orientation. This approach, in addition to reducing the calculation effort required, offers greater reliability than any calculation of accumulated wetting half-days.
- In turn, a general equation has been provided that (preliminarily) enables the establishment of a direct extrapolation between this number of expected wetting half-days and the $I_{A\theta}$ value (mm/year) obtained by the reference method.

In addition, it has been found that the wind speed threshold established by the alternative method to define a wetting half-day (> 2 m/s) can constitute an obstacle to the correct characterisation of the WDR exposure in locations with a low wind exposure. In this sense, it is still pending to identify those thresholds of precipitation, wind speed and relative humidity that would improve the equivalence of the alternative method (and their variability depending on the site's climate). Additionally, to consider the influence of new climatic variables such as temperature or solar radiation on moisture evaporation in façades, and even analyse wind direction records within $\pm 90^\circ$ of the perpendicular to the façade orientation θ (instead of the current $\pm 60^\circ$) represent a broad field of research for the future scope of the present study.

6. Conclusions

The continuous improvement of international standards is a task of great interest in the respective fields in which these standards are applied and a challenge for researchers. The alternative method supported by the international standard ISO 15927-3 provides a necessary tool to characterise the WDR exposure in locations without exhaustive hourly climatic data. This research has demonstrated the need to reformulate this alternative method—not only to clarify its calculation methodology but also to improve its reliability and accuracy. By analysing the results obtained through different methodological interpretations, an

improvement for this method that is capable of increasing its general convergence with respect to the reference method based on hourly climate data has been proposed.

The reanalysis performed on a representative number of façade locations and orientations subjected to different WDR exposures confirms that the proposed reformulation would enable (i) a more precise characterisation of the WDR exposure from average wind records and the present weather code and (ii) the establishment of general extrapolations that allow calculation of the $I_{A\theta}$ values with reasonable accuracy from the results of the reformulated alternative method.

The proposed methodology change, based on the simple calculation of the expected yearly number of wetting half-days for a 10-year return period at each location and façade orientation (without any cumulative sum), constitutes an essential and necessary improvement for the standard ISO 15927-3. This minimises the uncertainty associated with a calculation procedure supported by an international standard. Its implementation enables a simpler calculation and a more reliable characterisation of the WDR exposure in locations with limited climatic records, thus enabling the use of more appropriate building façade designs in these locations.

Acknowledgements

This research was partially funded by the Foundation for the Promotion of Applied Scientific Research and Technology in Asturias (FICYT) through the GRUPIN project Ref. IDI/2018/000221, and The Spanish Ministry of Science, Innovation and Universities through the State Plan for Scientific and Technical Research and Innovation with the project Ref. PGC2018-098459-B-I00, both co-financed with EU FEDER funds. The authors acknowledge engineer Francisco J. Simón Polo for his help with data collection and processing.

References

- [1] P. Johansson, T. Svensson, A. Erkstrand-Tobin, Validation of critical moisture conditions for mould growth on building materials, *Build. Environ.* 62 (2013) 201-209. <https://doi.org/10.1016/j.buildenv.2013.01.012>
- [2] C. Hall, W.D. Hoff, *Water transport in brick, stone and concrete*, second ed., Spon Press, New York, 2012.
- [3] A. Erkal, D. D'Ayala, L. Sequeira, Assessment of wind-driven rain impact, related surface erosion and surface strength reduction of historic building materials, *Build. Environ.* 57 (2012) 336–348.
<https://doi.org/10.1016/j.buildenv.2012.05.004>
- [4] V. Kočí, E. Vejmelková, M. Čáchová, D. Koňáková, M. Keppert, J. Maděra, R. Černý, 2017. Effect of moisture content on thermal properties of porous building materials, *Int. J. Thermophys.* 38:28.
<https://doi.org/10.1007/s10765-016-2164-8>
- [5] M. Abuku, H. Janssen, S. Roels, Impact of wind-driven rain on historic brick wall buildings in a moderately cold and humid climate: Numerical analyses of mould growth risk, indoor climate and energy consumption, *Energ. Buildings.* 41-1 (2009) 101-110. <https://doi.org/10.1016/j.enbuild.2008.07.011>
- [6] D. D'Ayala, Y.D. Aktas, Moisture dynamics in the masonry fabric of historic buildings subjected to wind-driven rain and flooding, *Build. Environ.* 104 (2016) 208-220. <https://doi.org/10.1016/j.buildenv.2016.05.015>
- [7] L. Traversetti, F. Bartoli, G. Caneva, Wind-driven rain as a bioclimatic factor affecting the biological colonization at the archaeological site of Pompeii, Italy. *Int. Biodeter. Biodegr.* 134 (2018) 31-38.
<https://doi.org/10.1016/j.ibiod.2018.07.016>
- [8] O. Ortega, J.L. Montero, J.A. Baptista, I.B. Beech, J. Sunner, C. Gaylarde, Deterioration and microbial colonization of cultural heritage stone buildings in polluted and unpolluted tropical and subtropical climates: A meta-analysis, *Int. Biodeter. Biodegr.* 143 (2019) 104734. <https://doi.org/10.1016/j.ibiod.2019.104734>
- [9] B. Blocken, J. Carmeliet, A review of wind-driven rain research in building science, *J. Wind. Eng. Ind. Aerodyn.* 92-13 (2004) 1079–1130. <https://doi.org/10.1016/j.jweia.2004.06.003>

- [10] S.M. Cornick, M.A. Lacasse, A review of climate loads relevant to assessing the watertightness performance of walls, windows and wall-window interfaces, *J. ASTM. Int.* 2-10 (2005) 1-15.
<https://doi.org/10.1520/JAI12505>.
- [11] EN ISO 15927-3, Hygrothermal performance of buildings. Calculation and presentation of climatic data. Part 3: calculation of a driving rain index for vertical surfaces from hourly wind and rain data, European Committee for Standardization, Brussels, 2009.
- [12] M. Kalousek, M. Jakubcik, Comparison of driving rain index calculated according to EN 15927-3 to the CFD simulation and experimental measurement, *Appl. Mech. Mater.* 861 (2016) 239-246.
<https://doi.org/10.4028/www.scientific.net/AMM.861.239>
- [13] S.A. Orr, M. Young, D. Stelfox, J. Curran, H. Viles, Wind-driven rain and future risk to built heritage in the United Kingdom: Novel metrics for characterising rain spells, *Sci. Total Environ.* 640-641C (2018) 1098-1111.
<https://doi.org/10.1016/j.scitotenv.2018.05.354>
- [14] H. Ge, U.K. Deb Nath, V. Chiu, Field measurements of wind-driven rain on mid-and high-rise buildings in three Canadian regions, *Build. Environ.* 116 (2017) 228-245. <http://dx.doi.org/10.1016/j.buildenv.2017.02.016>
- [15] S.A. Orr, H. Viles, Characterisation of building exposure to wind-driven rain in the UK and evaluation of current standards, *J. Wind. Eng. Ind. Aerodyn.* 180 (2018) 88-97. <https://doi.org/10.1016/j.jweia.2018.07.013>
- [16] BS 8104:1992, Code of practice for assessing exposure of walls to wind-driven rain, British Standards Institution, London, 1992.
- [17] WMO, Manual on Codes. International Codes (WMO-No. 306), Annex World Meteorological Organization, Geneva, 2018.
- [18] C. Sanders, Comparison of the 'British standard' and 'French' methods for estimating driving rain impacts on walls; IEA Annex 41 - Glasgow Meeting, International Energy Agency, Glasgow, 2004.

- [19] Met Office (United Kingdom's national weather service), UK actual and anomaly maps.
<https://www.metoffice.gov.uk/climate/uk/summaries/anomacts>, 2019 (accessed 26 November 2019).
- [20] M.C. Peel, B.L. Finlayson, T.A. McMahon, Updated world map of the Köppen-Geiger climate classification, *Hydrol. Earth. Syst. Sci.* 11 (2007) 1633-1644. <https://doi.org/10.5194/hess-11-1633-2007>
- [21] National Center for Geographic Information, National Atlas of Spain - Section II: The land environment, climatology. <http://www.ign.es/ane/ane1986-2008/>, 2019 (accessed 26 November 2019).
- [22] S. Hoppestad, Slagregninorge (Driving rain in Norway, in Norwegian); NBI Report no. 13, Norwegian Building Research Institute, Oslo: 1955.
- [23] R.E. Lacy, H.C. Shellard, An index of driving rain, *Meteorol. Mag.* 91-1080 (1962) 177–184.
- [24] J.F. Straube, E.F.P. Burnett, Simplified prediction of driving rain deposition, in: Proceedings of international building physics conference, Eindhoven, 2000, pp. 375–382.
- [25] R.E. Lacy, Driving-rain index (Building Research Establishment report), Department of the Environment, London, 1976.
- [26] R.E. Lacy, Driving-rain maps and the onslaught of rain on buildings, in: Proceedings of RILEM/CIB symposium on moisture problems in buildings, Helsinki, 1965.
- [27] R.E. Lacy, Climate and building in Britain, Her Majesty's Stationery Office, London, 1977.
- [28] WMO, Guide to Meteorological instruments and methods of observation (WMO-No 8), World Meteorological Organization, Geneva, 2008.
- [29] R.L. Smith Extreme value theory, in: W. Ledermann (Ed.), *Handbook of Applicable Mathematics*, John Wiley, Chichester, 1990, pp. 437-471.
- [30] E.J. Gumbel, The return period of flood flows, *Ann. Math. Stat.* 12-2 (1941) 163–190.
<https://doi.org/10.1214/aoms/1177731747>.

- [31] J.M. Pérez, J. Domínguez, B. Rodríguez, J.J. del Coz, E. Cano, Optimised method for estimating directional driving rain from synoptic observation data, *J. Wind. Eng. Ind. Aerodyn.* 113 (2013) 1-11.
<http://dx.doi.org/10.1016/j.jweia.2012.12.001>
- [32] B. Blocken, J. Carmeliet, Overview of three state-of-the-art wind-driven rain assessment models and comparison based on model theory, *Build. Environ.* 45-3 (2010) 691–703.
<https://doi.org/10.1016/j.buildenv.2009.08.007>
- [33] E.J. Gumbel, *Statistics of Extremes*, Columbia University Press, New York, 1958.
- [34] S. Nadarajah, The exponentiated Gumbel distribution with climate application, *Environmetrics* 17-1 (2006) 13-23. <https://doi.org/10.1002/env.739>
- [35] J.L. Devore, *Probability & Statistics for Engineering and the Sciences*, eighth ed., Cengage Learning, Boston, 2010.
- [36] Government of Canarias, Agroclimatic data.
http://www.gobiernodecanarias.org/agricultura/agricultura/temas/datos_agroclimaticos/estaciones.html, 2019 (accessed 26 November 2019).
- [37] V. Masson, P. Bougeault, Numerical simulation of a low-level wind created by complex orography: a Cierzo case study, *Mon. Weather. Rev.* 124-4 (1996) 701-715. [https://doi.org/10.1175/1520-0493\(1996\)124<0701:NSOALL>2.0.CO;2](https://doi.org/10.1175/1520-0493(1996)124<0701:NSOALL>2.0.CO;2)
- [38] Government of La Rioja, Agroclimatic information (Customised search).
<https://www.larioja.org/agricultura/es/informacion-agroclimatica/consulta-personalizada>, 2019 (accessed 26 November 2019).
- [39] J.M. Pérez, J. Domínguez, E. Cano, J.J. del Coz, F.P. Álvarez, On the significance of the climate-dataset time resolution in characterising wind-driven rain and simultaneous wind pressure. Part II: directional analysis, *Stoch. Environ. Res. Risk. Assess.* 32 (2018) 1799–1815. <https://doi.org/10.1007/s00477-017-1480-2>

[40] Xunta de Galicia, Meteogalicia - Meteorological reports (Data Access).

https://www.meteogalicia.gal/observacion/rede/redeIndex.action?request_locale=es, 2019 (accessed 26 November 2019).

List of tables

Table 1. Summary of the methodological interpretations considered for the reanalysis of the alternative method.

Table 2. Example of the summary of the highest annual I'_{S0} values at the Calahorra station and the Gumbel distribution parameters required for the calculation of the I_{S0} reference value.

Table 1.

Summary of the methodological interpretations considered for the reanalysis of the alternative method.

	Guideline to consider a wetting period finished*	Methodology justification
Original validation	It ends when a single drying half-day occur	Originally used to validate the alternative method (IEA-Annex 41 and Informative Annex D of ISO standard)
Interpretation A	It ends before 8 non-wetting half-days occur	Similar approach to the spell of the reference method
Interpretation B	It ends when the cumulative sum returns to 0 and in any case, at the beginning of a new year	An opposite and cumulative effect of wetting and drying half-days is considered

() The value of the cumulative series resets to 0, until the beginning of a new wetting period (occurrence of a +1 value). The cumulative sum has a minimum value of 0.*

Table 2.

Example of the summary of the highest annual $I'_{S\theta}$ values at the Calahorra station and the Gumbel distribution parameters required for the calculation of the $I_{S\theta}$ reference value.

Calahorra station (La Rioja): North orientation (0°/360°)			
42.33408° / -2.00188° (Decimal Degrees)			
Year	Máximo $I'_{S\theta}$ value (mm/spell)	Year	Máximo $I'_{S\theta}$ value (mm/spell)
2008	21.562	2013	32.918
2009	16.145	2014	25.795
2010	7.799	2015	18.382
2011	5.652	2016	16.588
2012	17.996	2017	11.433
Magnitude	Value	Comment	
N	10	Number of x_i data (2008-2017).	
\bar{x}	17.4271	Data average: $\bar{x} = \sum x_i / N$	
σ_x	7.7328	Standard deviation: $\sigma_x = \sqrt{\sum (x_i - \bar{x})^2 / N}$	
u_y	0.4952	Data average of 1 to N y_i values (reduced variable): $y_i = -\ln(\ln(N + 1/i))$ (Only depends on N value)	
σ_y	0.9496	Standard deviation of 1 to N y_i values (reduced variable): $y_i = -\ln(\ln(N + 1/i))$ (Only depends on N value)	
u_x	13.3946	Mode: $u = \bar{x} - u_y \frac{\sigma_x}{\sigma_y}$	
β_x	8.1430	Dispersion parameter: $\beta = \frac{\sigma_x}{\sigma_y}$	
$I_{S\theta}$	20.7455	Reference value associated with a 3-year return period (Eq. 4)	

Figure captions

Figure 1. Coefficients of determination identified for the original validation carried out in London (Heathrow), Manchester (Ringway), and Edinburgh (Turnhouse). *Data obtained from IEA-Annex 41 and verified with Figures D.1 and D.2 of ISO standard 15927-3.*

Figure 2. Accumulated wetting half-days on a specific façade of Pazuengos (La Rioja) during 2008, considering three different interpretations for the wetting period length. The periods end on a drying half-day (original validation in ISO annex); A) upon 8 non-wetting half-days; and B) when the number of drying and wetting half-days are equal.

Figure 3. WDR exposure results based on hourly climatic data ($I_{A\theta}$ and $I_{S\theta}$ values) for the 12 analysed weather stations (degrees from the North): Canary Islands (top), La Rioja (centre), and Galicia (bottom). Their main characteristics and locations are also shown.

Figure 4. WDR exposure characterisation based on different interpretations of the alternative method (accumulated wetting half-days), for the 12 Spanish weather stations (*degrees from the North*).

Figure 5. Coefficients of determination identified for the 12 analysed weather stations by applying the original approach supported by Informative Annex D of ISO 15927-3.

Figure 6. Coefficients of determination identified for the 12 analysed weather stations by applying Interpretation A.

Figure 7. Coefficients of determination identified for the 12 analysed weather stations by applying Interpretation B.

Figure 8. Coefficients of determination identified in the 12 analysed weather stations by considering the expected annual number of wetting half-days for a 10-year return period.

Figure 1

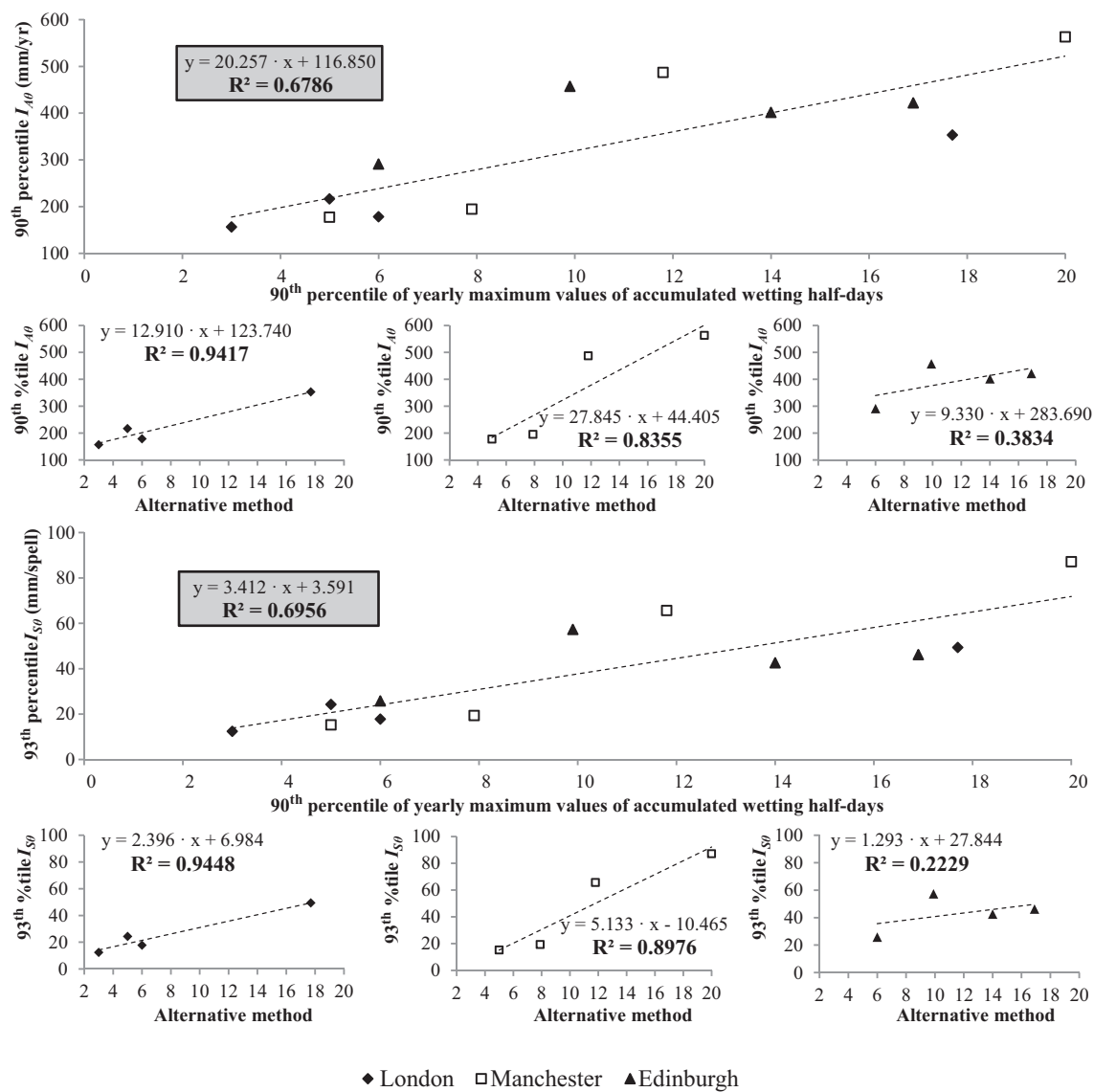


Fig. 1. Coefficients of determination identified for the original validation carried out in London (Heathrow), Manchester (Ringway), and Edinburgh (Turnhouse). Data obtained from IEA-Annex 41 and verified with Figures D.1 and D.2 of ISO standard 15927-3.

Figure 2

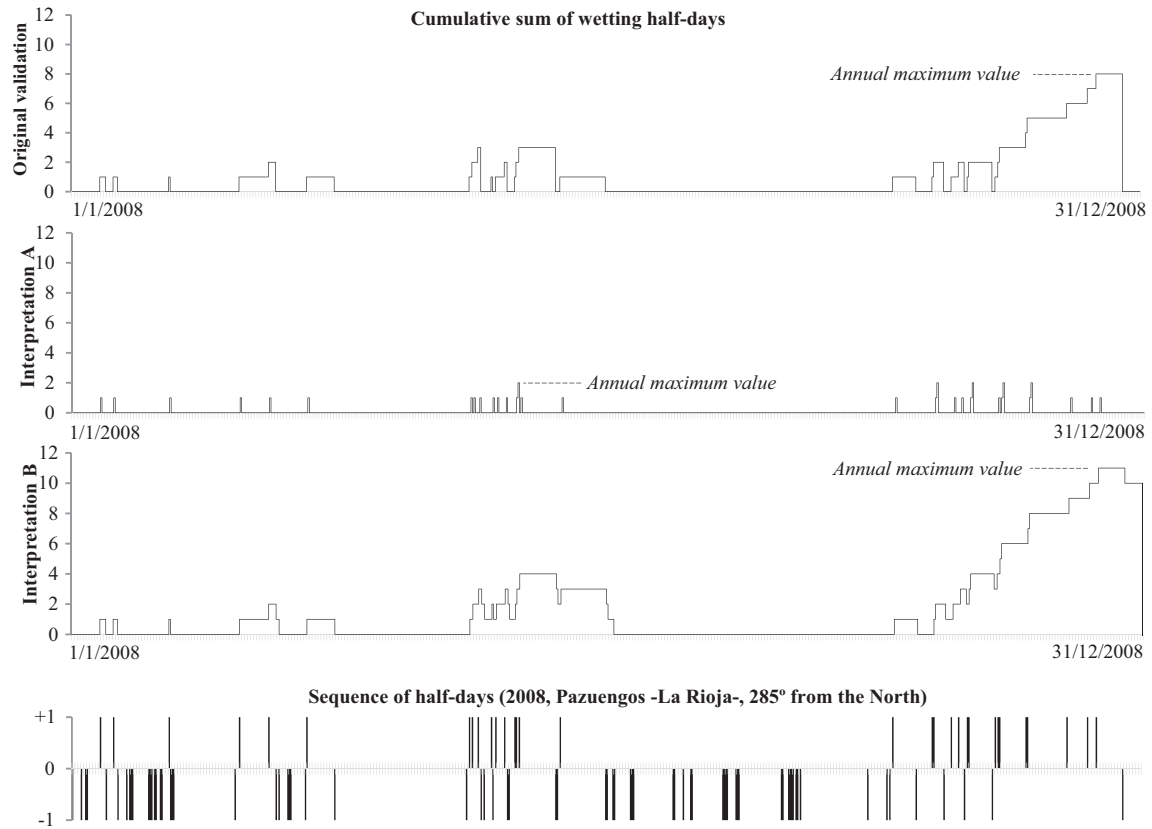


Fig. 2. Accumulated wetting half-days on a specific facade of Pazuengos (La Rioja) during 2008, considering three different interpretations for the wetting period length. The periods end on a drying half day (original validation in ISO annex); A) upon 8 non-wetting half-days; and B) when the number of drying and wetting half-days are equal.

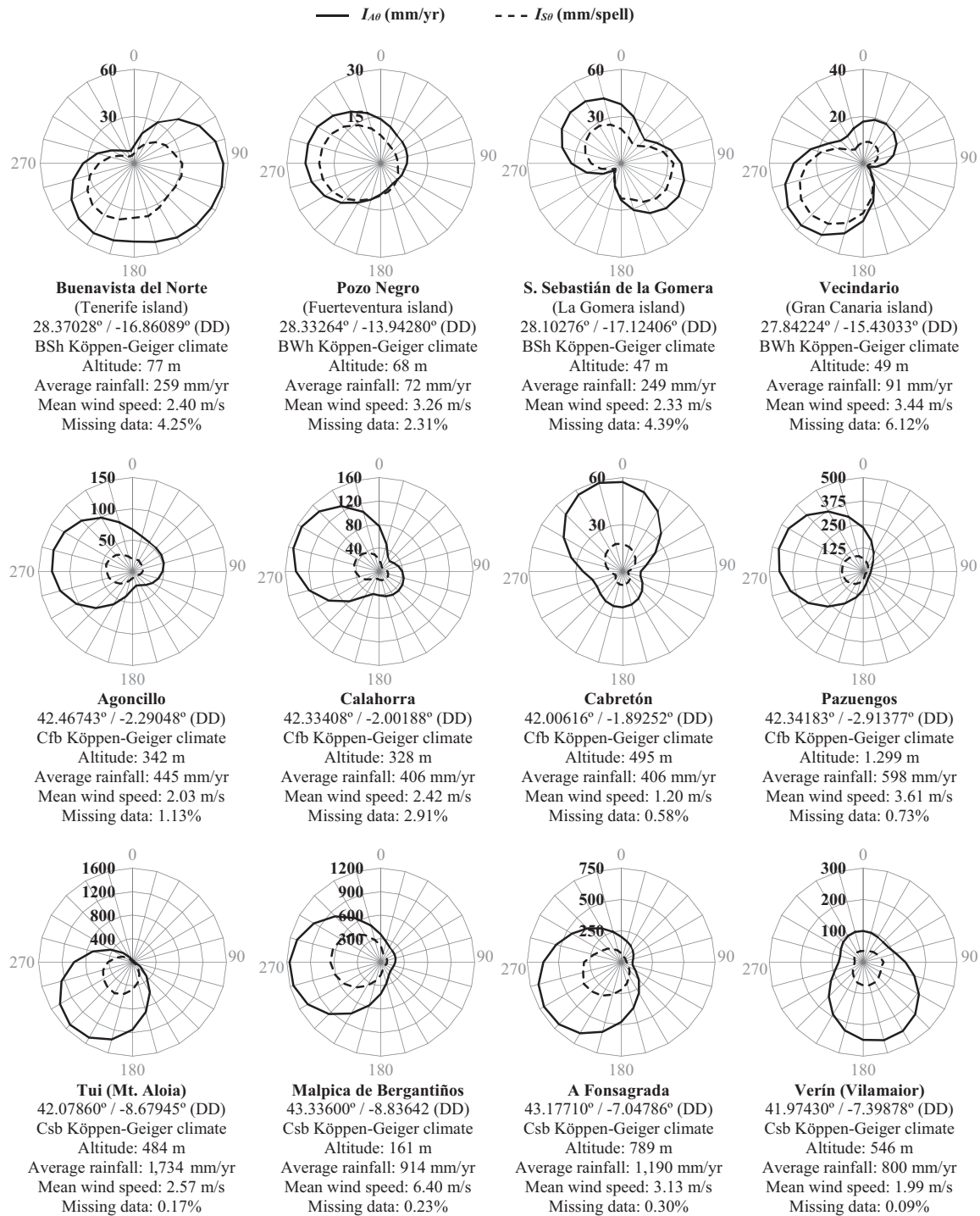


Fig. 3. WDR exposure results based on hourly climatic data (I_{A0} and I_{S0} values) for the 12 analysed weather stations (*degrees from the North*): Canary Islands (top), La Rioja (center), and Galicia (bottom). Their main characteristics and locations are also shown.

Figure 4

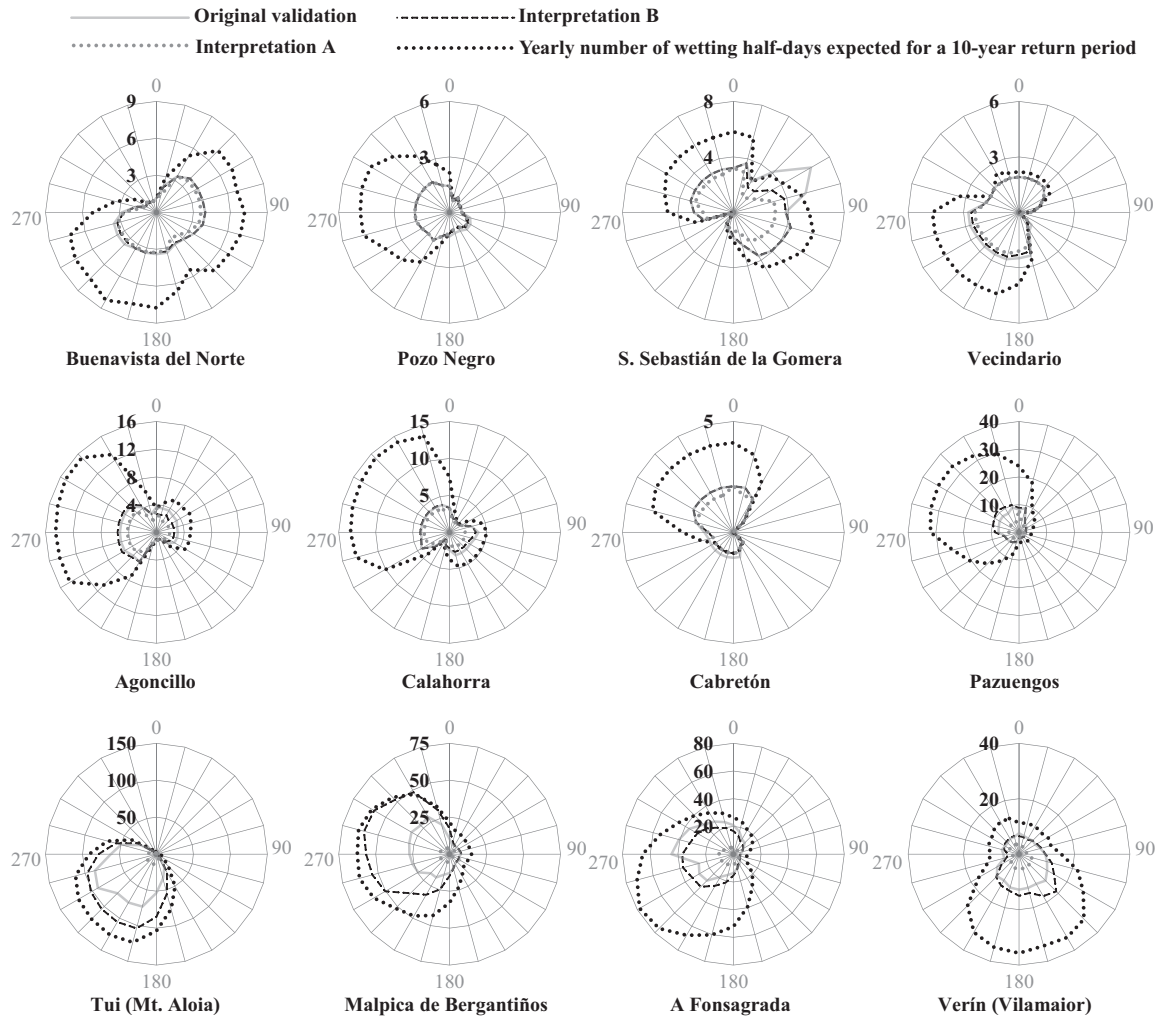
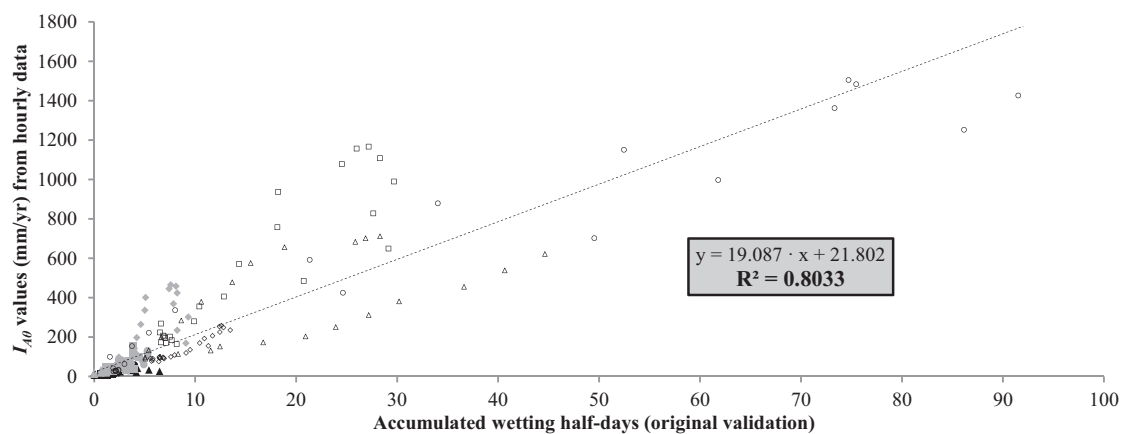
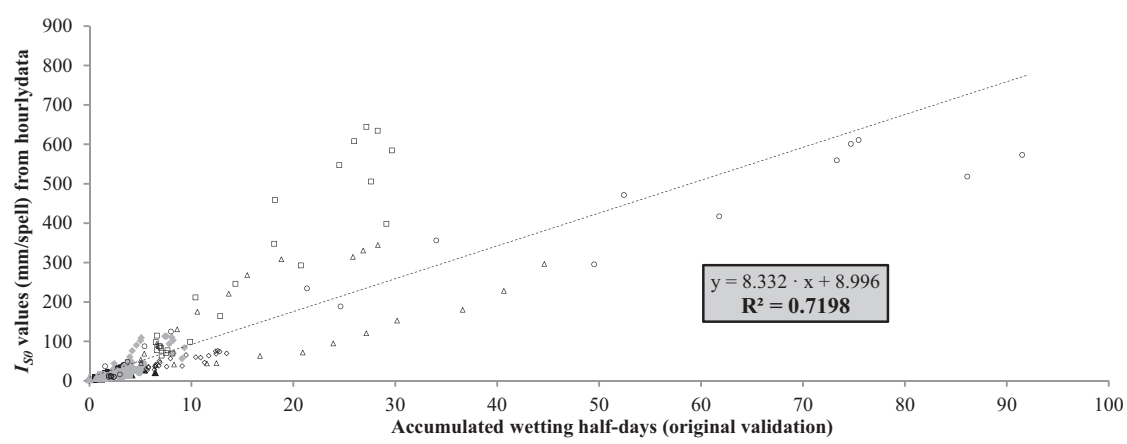


Fig. 4. WDR exposure characterisation based on different interpretations of the alternative method (accumulated wetting half-days), for the 12 Spanish weather stations (degrees from the North).

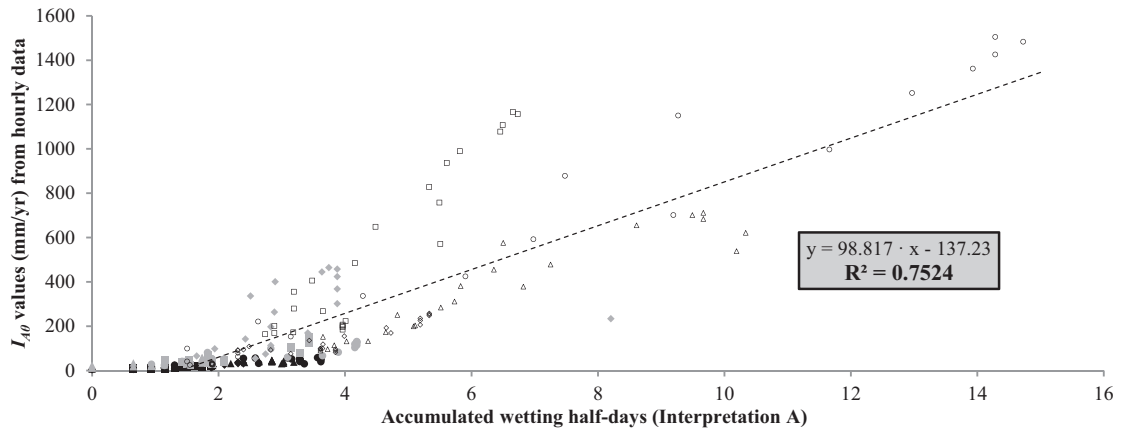


Station (Canary Islands)	R ²	Station (La Rioja)	R ²	Station Galicia)	R ²
● Buenavista del Norte	0.8168	● Agoncillo	0.7663	○ Tui (Mt. Aloia)	0.9445
■ Pozo Negro	0.6782	■ Calahorra	0.4613	□ Malpica de Bergantiños	0.8338
▲ S. Sebastián de la Gomera	0.3670	▲ Cabretón	0.7248	△ A Fonsagrada	0.4591
◆ Vecindario	0.7645	◆ Pazuengos	0.6322	◇ Verín (Vilamaior)	0.9223
Average R² value (goodness-of-fit)		0.6976			

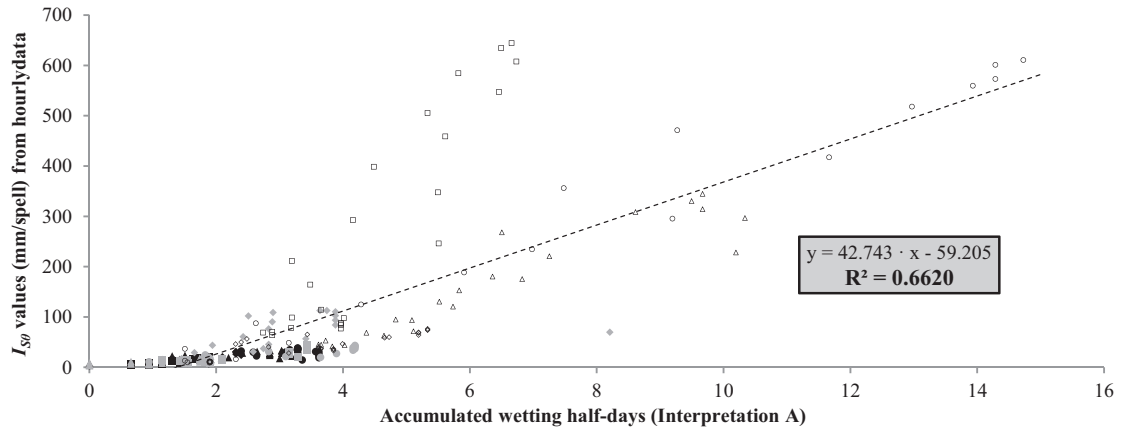


Station (Canary Islands)	R ²	Station (La Rioja)	R ²	Station Galicia)	R ²
● Buenavista del Norte	0.6773	● Agoncillo	0.7765	○ Tui (Mt. Aloia)	0.9496
■ Pozo Negro	0.8078	■ Calahorra	0.5176	□ Malpica de Bergantiños	0.9028
▲ S. Sebastián de la Gomera	0.4611	▲ Cabretón	0.6903	△ A Fonsagrada	0.3754
◆ Vecindario	0.6810	◆ Pazuengos	0.5908	◇ Verín (Vilamaior)	0.8048
Average R² value (goodness-of-fit)		0.6863			

Fig. 5. Coefficients of determination identified for the 12 analysed weather stations by applying the original approach supported by Informative Annex D of ISO 15927-3.

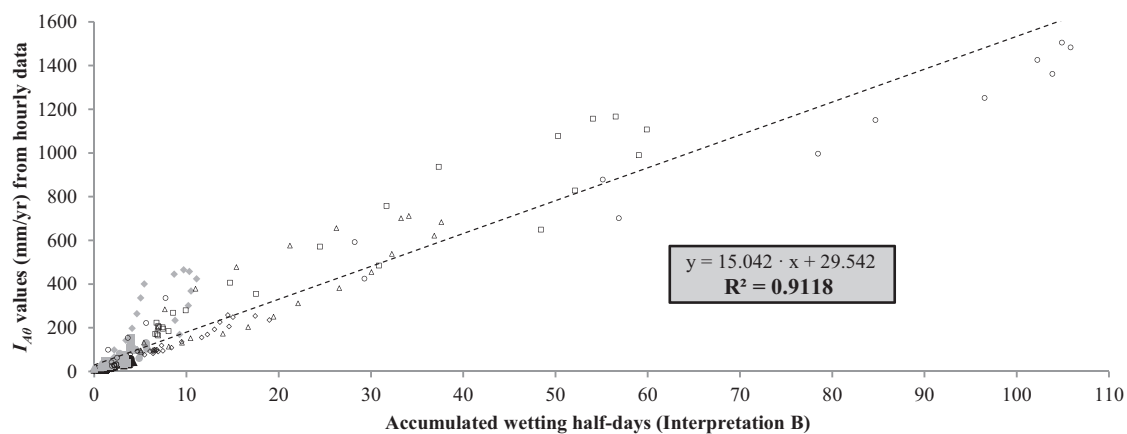


Station (Canary Islands)	R ²	Station (La Rioja)	R ²	Station Galicia)	R ²
• Buenavista del Norte	0.7541	• Agoncillo	0.8327	◊ Tui (Mt. Aloia)	0.9724
■ Pozo Negro	0.7865	■ Calahorra	0.8141	◻ Malpica de Bergantiños	0.8832
▲ S. Sebastián de la Gomera	0.8132	▲ Cabretón	0.7389	△ A Fonsagrada	0.8929
◆ Vecindario	0.7152	◆ Pazuengos	0.2796	◊ Verín (Vilamaior)	0.7728
Average R² value (goodness-of-fit)		0.7713			

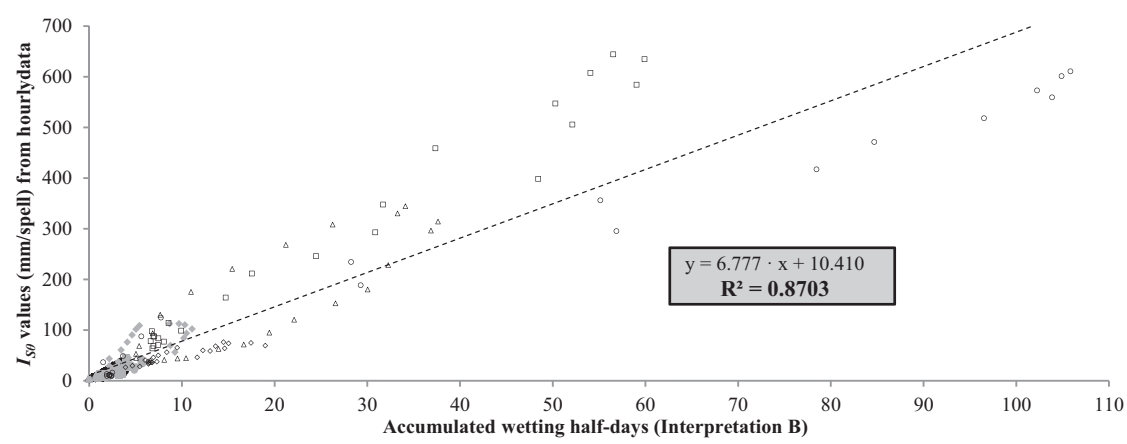


Station (Canary Islands)	R ²	Station (La Rioja)	R ²	Station Galicia)	R ²
• Buenavista del Norte	0.6421	• Agoncillo	0.8224	◊ Tui (Mt. Aloia)	0.9750
■ Pozo Negro	0.8566	■ Calahorra	0.8169	◻ Malpica de Bergantiños	0.8365
▲ S. Sebastián de la Gomera	0.6839	▲ Cabretón	0.7090	△ A Fonsagrada	0.8856
◆ Vecindario	0.5673	◆ Pazuengos	0.2751	◊ Verín (Vilamaior)	0.5182
Average R² value (goodness-of-fit)		0.7157			

Fig. 6. Coefficients of determination identified for the 12 analysed weather stations by applying Interpretation A.



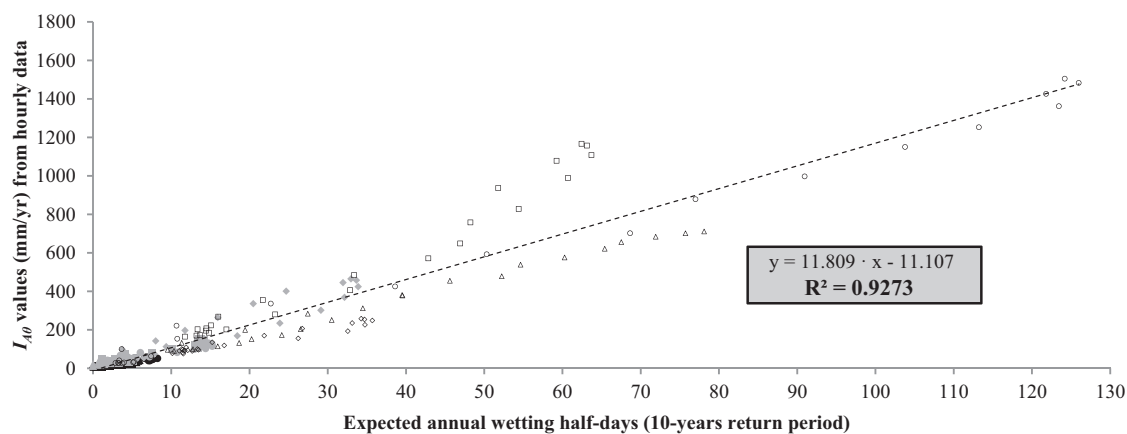
Station (Canary Islands)	R ²	Station (La Rioja)	R ²	Station Galicia)	R ²
● Buenavista del Norte	0.8230	● Agoncillo	0.8562	○ Tui (Mt. Aloia)	0.9810
■ Pozo Negro	0.7865	■ Calahorra	0.6240	□ Malpica de Bergantiños	0.9208
▲ S. Sebastián de la Gomera	0.7695	▲ Cabretón	0.8038	△ A Fonsagrada	0.7867
◆ Vecindario	0.7580	◆ Pazuengos	0.7086	◇ Verín (Vilamaior)	0.9196
Average R² value (goodness-of-fit)		0.8115			



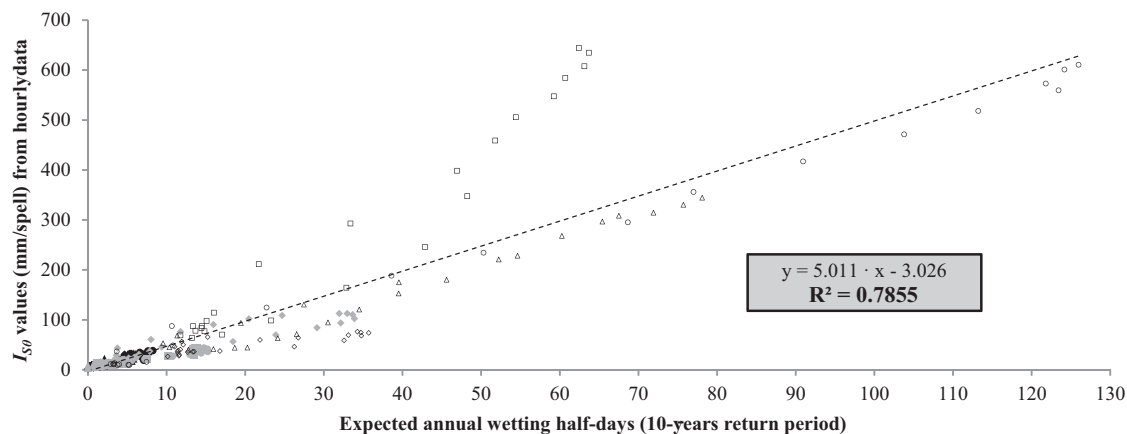
Station (Canary Islands)	R ²	Station (La Rioja)	R ²	Station Galicia)	R ²
● Buenavista del Norte	0.6489	● Agoncillo	0.8658	○ Tui (Mt. Aloia)	0.9854
■ Pozo Negro	0.8566	■ Calahorra	0.6526	□ Malpica de Bergantiños	0.9742
▲ S. Sebastián de la Gomera	0.7913	▲ Cabretón	0.7648	△ A Fonsagrada	0.7132
◆ Vecindario	0.6357	◆ Pazuengos	0.6189	◇ Verín (Vilamaior)	0.8231
Average R² value (goodness-of-fit)		0.7775			

Fig. 7. Coefficients of determination identified for the 12 analysed weather stations by applying Interpretation B.

Figure 8



Station (Canary Islands)	R ²	Station (La Rioja)	R ²	Station Galicia)	R ²
• Buenavista del Norte	0.8563	● Agoncillo	0.9172	○ Tui (Mt. Aloia)	0.9935
■ Pozo Negro	0.9444	■ Calahorra	0.9060	□ Malpica de Bergantiños	0.9677
▲ S. Sebastián de la Gomera	0.8695	▲ Cabretón	0.8280	△ A Fonsagrada	0.9874
◆ Vecindario	0.9297	◆ Pazuengos	0.9197	◇ Verín (Vilamaior)	0.9513
Average R² value (goodness-of-fit)		0.9226			



Station (Canary Islands)	R ²	Station (La Rioja)	R ²	Station Galicia)	R ²
• Buenavista del Norte	0.8499	● Agoncillo	0.9187	○ Tui (Mt. Aloia)	0.9956
■ Pozo Negro	0.9432	■ Calahorra	0.9174	□ Malpica de Bergantiños	0.9505
▲ S. Sebastián de la Gomera	0.7076	▲ Cabretón	0.7681	△ A Fonsagrada	0.9665
◆ Vecindario	0.8982	◆ Pazuengos	0.8309	◇ Verín (Vilamaior)	0.7097
Average R² value (goodness-of-fit)		0.8714			

Fig. 8. Coefficients of determination identified in the 12 analysed weather stations by considering the expected annual number of wetting half-days for a 10-year return period.